

# COMPATIBILITY OF FRACTURE MECHANICS PARAMETERS AND FATIGUE CRACK GROWTH PARAMETERS IN WELDED JOINT BEHAVIOUR EVALUATION

*Ivica Čamagić, Nemanja Vasić, Zlatibor Vasić, Zijah Burzić, Aleksandar Sedmak*

Original scientific paper

Problem of fracture toughness,  $K_{Ic}$ , determination on a crack tip localized in a welded joint is set in principle, since fracture mechanics presumes homogeneous material, not only in a crack tip surrounding but on a distance from it, in order to maintain valid the theoretical presumptions and the meaning of the fracture toughness as a property measured by some of the fracture mechanics methods. Welded joint represents the non-homogeneity by its microstructure and mechanical properties, often by geometrical form, and by stress field as well, which are affected by different factors as well as residual stress after welding. Safety of a welded joint submitted to a variable load is a dominant topic of all serious researches in this area nowadays, thus a part of research in this paper is aimed at the analysis of variable load influence on a welded joint behaviour in the presence of a crack type defect, or in other words to the determination of the fatigue crack growth parameters.

**Keywords:** crack, fatigue crack growth parameters, fracture toughness, welded joint

## Kompatibilnost parametara mehanike loma i parametara rasta zamorne pukotine u ocjeni ponašanja zavarenih spojeva

Izvorni znanstveni članak

Problem određivanja žilavosti loma,  $K_{Ic}$ , na vrhu pukotine lokalizirane u zavarenom spoju postavlja se načelno, zbog toga što mehanika loma pretpostavlja homogen materijal, ne samo u okolini vrha pukotine već i na udaljenosti od njega, kako bi ostale u važnosti teorijske pretpostavke i značenje žilavosti loma kao svojstva izmjerene nekom od metoda mehanike loma. Zavareni spoj predstavlja nehomogenost po mikrostrukтури i mehaničkim svojstvima, često po geometrijskom obliku, a također i po polju naprezanja, na koje utječu razni faktori kao i zaostala naprezanja nakon zavarivanja. Sigurnost zavarenih spojeva pri djelovanju promjenjivog opterećenja je u današnje vrijeme dominantna tema svih ozbiljnijih istraživača u ovom području ispitivanja, tako da je dio istraživanja u okviru ovog rada usmjeren i na analizu utjecaja promjenjivog opterećenja na ponašanje zavarenog spoja u prisustvu greške tipa pukotine, odnosno određivanje parametara rasta zamorne pukotine.

**Ključne riječi:** parametri rasta zamorne pukotine, pukotina, zavareni spoj, žilavost loma

### 1 Introduction

High strength low alloyed steel, Nionikral 70, was chosen for the base metal and the welded joint behaviour testing. It was produced in an electric furnace, cast into blooms, and flat rolled to 18 mm thick slabs. Strengthening was done in combination of a classic improvement (quenching and tempering), followed by grain refinement due to adequately selected chemical composition, micro alloying and appropriate deposition. The mechanical properties and the chemical composition of the delivered sheet metal are given in Tab. 1 [1]. "ACRONI - Slovenske Železarne" Jesenice was the material supplier.

Tenacito 75, basic coated, low hydrogen electrode, in diameters of 3,25 and 4 mm, was chosen for the plates welding. The choice was made according to the base material properties and thickness and the chosen welding procedure [1], according to the ACRONI Jesenice catalogue recommendations. The mechanical properties and the chemical composition of the chosen electrode are given in Tab. 2 [1]. Welded joint is butt 2/3 X-weld. Groove preparation was done according to the SRPS EN ISO 9692-1:2012 [2].

### 2 Experimental determination of the fracture mechanics parameters

#### 2.1 Fracture toughness, $K_{Ic}$ , determination at plain strain

With the analysis of behaviour of a brittle solid with crack, fracture mechanics opened new possibilities for welded structures safety insurance. Process of linear-elastic fracture mechanics development is completed to its applicability on real constructions made from a high strength material, for a plane strain state in a crack presence, with the ASTM E399 [3] standard for a fracture toughness,  $K_{Ic}$ , determination under plain deformation. Condition for the testing validity is that plastic deformation engages only negligible small area round crack tip before crack propagation and fracture occurs. Since large area of plastic deformation forms around crack tip with majority of structural materials and welded joints, direct determination of parameter  $K_{Ic}$  is not possible, and its application in real conditions is limited.

Analysis of plastic behaviour of a material, as an interest of elastic-plastic fracture mechanics, lead to the definition of the two following parameters:

- Crack tip opening displacement CTOD ( $\delta$ ), and
- Contour  $J$  integral, independent of integration path.

**Table 1** Mechanical properties and chemical composition of Nionikral 70 steel

Batch	Testing direction		Yield strength $R_{p0,2}$ / MPa, min.			Tensile strength $R_m$ / MPa, min.			Dilatation $\varepsilon$ / %	
180079	L - T		710			770			14	
% mass share of alloying elements										
C	Si	Mn	P	S	Cr	Ni	Mo	V	Al	
0,10	0,20	0,23	0,009	0,018	1,24	3,10	0,29	0,05	0,08	

**Table 2** Mechanical properties and chemical composition of Tenacito 75 electrode

Electrode	Yield strength $R_{p0,2}$ / MPa, min	Tensile strength $R_m$ / MPa, min.	Dilatation $\epsilon$ / %	Impact energy / J		
				-20 °C	-40 °C	-60 °C
Tenacito 75	725	780	12	110 ÷ 140	65 ÷ 95	50 ÷ 80
% mass share of alloying elements						
C	Mn	Si	Cr	Ni	Mo	
0,06	1,45	0,25	0,55	2,0	0,35	

In the linear-elastic area these two parameters are directly connected with the  $K_{Ic}$  value and they present the critical values for which the strain deformation conditions are satisfied:

$$CTOD_c = \delta_{Ic} = \frac{(1-\nu^2) \cdot K_{Ic}^2}{E \cdot \lambda \cdot R_{p0,2}} \tag{1}$$

$$J_{Ic} = \frac{(1-\nu^2) \cdot K_{Ic}^2}{E} = \lambda \cdot R_{p0,2} \cdot \delta_{Ic} \tag{2}$$

where:

$E$  – elastic modulus, MPa

$\nu$  – Poisson’s ratio, –

$R_{p0,2}$  – yield strength, MPa

$\lambda$  – factor of proportionality that equals from 1 to 2,6.

Applicability of CTOD and  $J$  parameters is in the possibility of their analysis even after development of significant plastic deformations, on one hand, and in the suitability for their experimental determination, regulated by the BS 5762 [4] standard for CTOD and the ASTM E813 [5] standard for  $J$  integral, on the other hand.

Fracture mechanics testing of specimens taken from welded plates made of Nionikral 70, was done in order to determine critical value of stress intensity factor,  $K_{Ic}$ . Specimens for three point bending (SEB) were used for testing. Their geometry is defined by the ASTM E399 [3] standard and it is shown in Fig. 1 [3 ÷ 7]. The specimen for three point bending has proved to be appropriate in practice, and thus it is used the most.

The testing itself was performed, at the room temperature, on the electro-mechanical testing machine SCHENCK TREBEL RM 100, shown in Fig. 2. Crack tip opening was registered by the special extensometer KLIP-GAGE DD1, whose measuring accuracy is  $\pm 0,001$  mm.

The fracture toughness,  $K_{Ic}$ , is determined based on the critical value of  $J$  integral, fracture toughness measure,  $J_{Ic}$ , by testing according to the ASTM E813-89 [5]. Testing method of a single specimen successive partial unload was used for the  $J$  integral determination. Points of the base dependency curve are obtained from the pair of data, acting force,  $F$ , crack tip opening,  $\delta$ . Construction of the resistance curve ( $J - \Delta a$  curve) is

requested by the procedure of the critical value determination of the fracture toughness measure,  $J_{Ic}$ , in which crack increment is determined based on the compliance alteration. From the obtained diagrams force  $F$  – crack tip opening  $\delta$ , two series of data were obtained by measuring and calculation:

- consumed work at individual stages of a cycle (area below the curve),
- compliance alteration (change of the slope of the elastic unload line).

Noticeable unloads on the  $F - \delta$  curve, serve for the specimen compliance determination, for the three point bending, at the current crack length  $a$ . From the compliance, which is represented by the ratio between  $\delta$  increment and  $F$  increment on unloading line, it is possible to determine crack length from the following:

$$\Delta a_i = \Delta a_{i-1} + \left( \frac{b_{i-1}}{2} \right) \cdot \left( \frac{C_{i-1} - C_i}{C_i} \right), \tag{3}$$

where:

$a_{i-1}$  – previous length of a crack,

$C_i = \tan \alpha_i$  – slope of the observed unloading line,

$C_{i-1} = \tan \alpha_{i-1}$  – slope of the previous unloading line.

Compliance was determined directly, by analog-digital plotter HP 7090A. Also,  $F - \delta$  diagrams were directly registered during the experiment, and they were the base for the calculation of all relevant parameters needed for the construction of the  $J - \Delta a$  curve.

$J$  integral was calculated from the following dependence:

$$J_i = \left[ J_{i-1} + \left( \frac{2}{b} \right) \cdot \frac{A_i - A_{i-1}}{B} \right] \cdot \left[ 1 - \frac{a_i - a_{i-1}}{b_i} \right], \tag{4}$$

where:

$A$  – area under the curve,

$B$  – specimen thickness,

$b$  – ligament length.

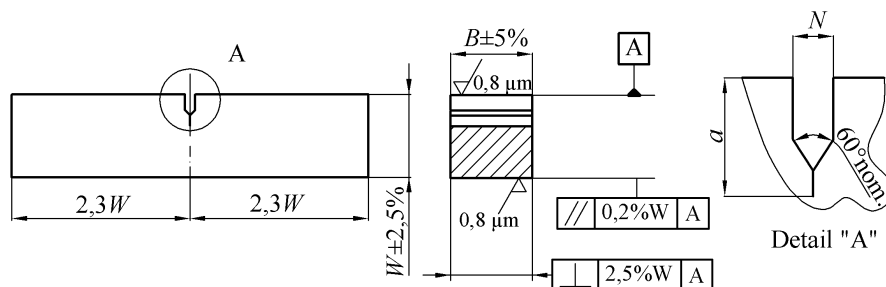


**Figure 1** Fracture mechanics testing specimen



Figure 2 Electro-mechanic testing machine SCHENCK-TREBEL RM 100

$F - \delta$  and  $J - \Delta a$  diagrams for specimens with a notch in base metal (BM), weld metal (WM) and heat affected zone (HAZ) are given in Figs. 3 to 5. The influence of the structure heterogeneity on the toughness properties of the welded joint components can be seen from the appearance of the diagrams themselves [1].

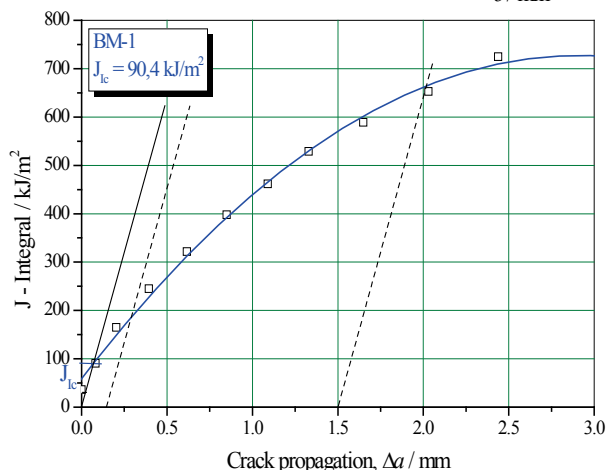
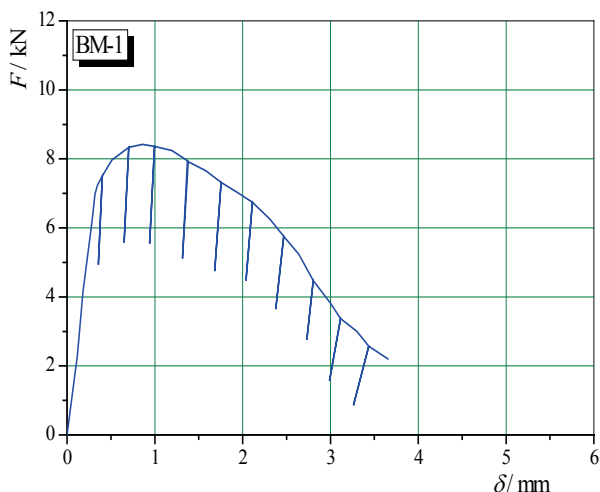


Figure 3  $F - \delta$  and  $J - \Delta a$  diagrams for a specimen with a notch in BM tested at the room temperature

Knowing the values of the critical  $J_{Ic}$  integral, the value of critical stress intensity factor or fracture toughness at plane strain,  $K_{Ic}$ , can be calculated according to:

$$K_{Ic} = \sqrt{\frac{J_{Ic} \cdot E}{1 - \nu^2}} \tag{5}$$

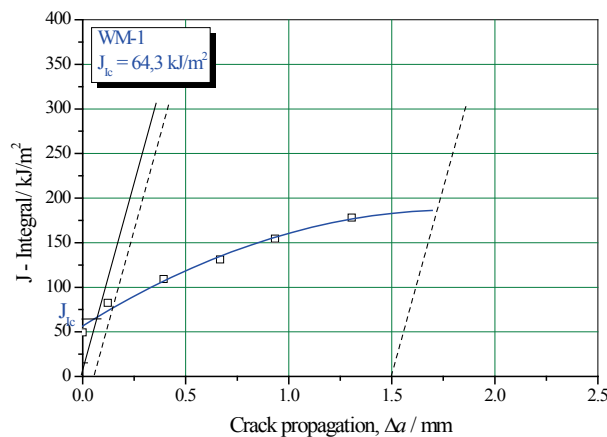
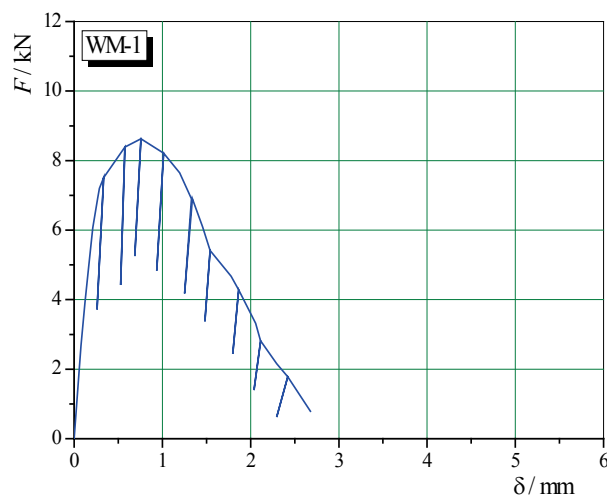


Figure 4  $F - \delta$  and  $J - \Delta a$  diagrams for a specimen with a notch in WM tested at the room temperature

Calculated values of the fracture toughness under the plane strain,  $K_{Ic}$ , are given in Tab. 3 [1].

Table 3 Values of the fracture mechanics parameters  $J_{Ic}$  and  $K_{Ic}$

Specimen mark	Critical $J$ integral $J_{Ic} / \text{kJ/m}^2$	Critical stress intensity factor $K_{Ic} / \text{MPa}\cdot\text{m}^{1/2}$
BM-1	90,4	142,7
BM-2	94,3	145,8
WM-1	64,3	119,2
WM-2	61,5	116,6
HAZ-1	80,4	131,9
HAZ-2	74,9	127,3

## 2.2 Determination of Fatigue Crack Propagation Parameter

The basic improvement that fracture mechanics brought in the field of the material fatigue is in analytical parse of the fracture phenomenon to the period of initiation, in which a fatigue crack initiates, and to the period of propagation or growth that follows and in which the initiated crack propagates to the critical size at which sudden fracture appears. Thus, the total number of cycles,  $N_t$ , after which fracture occurs, is divided to the number of cycles needed for a fatigue crack to initiate,  $N_i$ , and the number of cycles needed for it to propagate to the critical size for fracture,  $N_p$ .

$$N_t = N_i + N_p \tag{6}$$

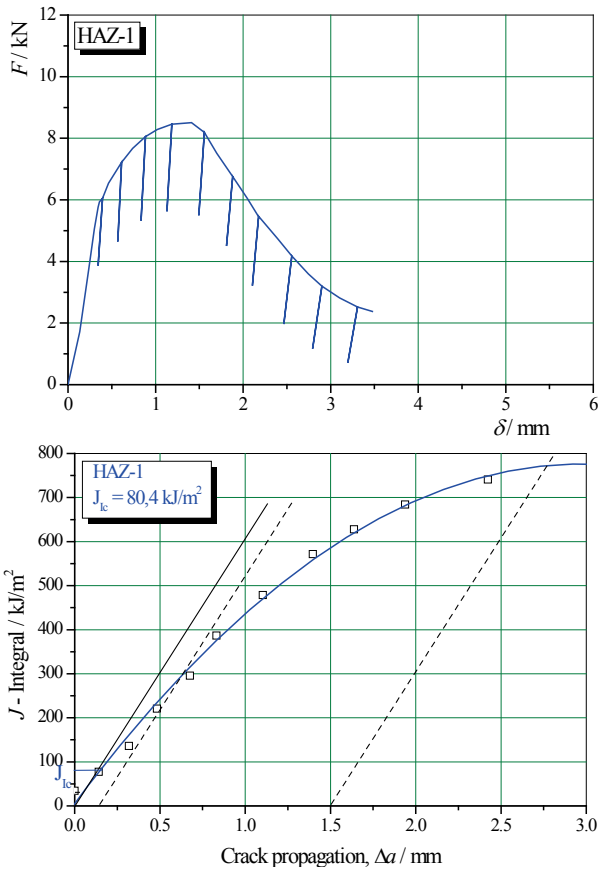


Figure 5  $F - \delta$  and  $J - \Delta a$  diagrams for a specimen with a notch in HAZ tested at the room temperature

The development in studying of material behaviour under the variable load influence is enabled by parallel introduction of experimental and theoretical approach, since only theoretical approach cannot fully explain the initiation and propagation of a fatigue crack. Intensive investigation is currently done in order to determine all the factors that affect the  $da/dN = f(\Delta K)$  dependence, in so called low-cycle fatigue, when plastic deformation occurs in the hysteresis loop of a single cycle. Application of linear-elastic fracture mechanics analysis procedures of stress and strain state on a propagating fatigue crack tip lead to the formulation of the Paris equation for all metals and alloys, which relates fatigue crack propagation rate with a crack tip stress intensity factor range [8]:

$$\frac{da}{dN} = C \cdot (\Delta K)^m \tag{7}$$

Although the Paris equation for a crack propagation is not valid in the entire area, between small rates near to the fatigue threshold ( $\Delta K_{th}$  shown in Fig. 6 [8]), and high rates ( $K_{Ic}$ ), large linear middle part of the curve covered by Paris relation has shown to be by far the most important from the practical point of view, since it simultaneously allows the difference to be made between fatigue crack initiation and propagation.

The testing, in order to determine fatigue crack propagation rate  $da/dN$  and fatigue threshold  $\Delta K_{th}$ , was performed at the room temperature, on standard Charpy

specimens, using the three point bending method, on a resonant high-frequency pulsator, shown in Fig. 7. The testing itself was performed within the force control. This pulsator achieves sinusoid alternate variable momentum load in the range from  $-70$  to  $70$  N·m. The device is connected with a computer, a printer and a plotter, which allows measuring automation and direct acquisition and processing of obtained data.

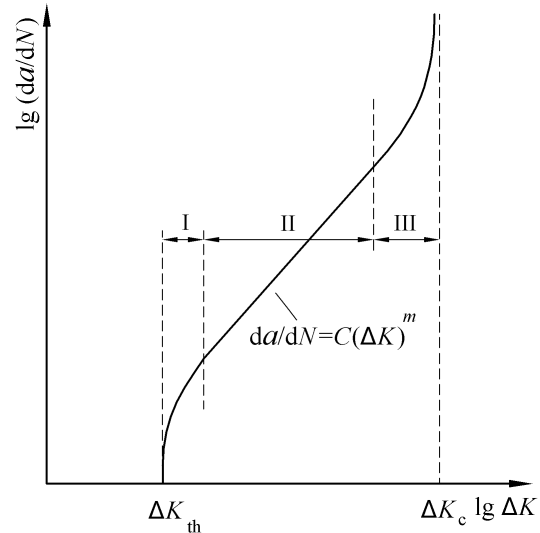


Figure 6 Typical curve of fatigue crack propagation rate in dependence on  $\Delta K$

The testing was performed for the same ratio of minimum and maximum load  $R = -1$ . Achieved frequency was in the range from 175 to 195 Hz, depending on whether the crack was going through base metal, weld metal or heat affected zone and size of the load. Mean load and its amplitude were registered with the accuracy of  $\pm 3$  N·cm.



Figure 7 High-frequency pulsator CRACKTRONIC

Specimens were mechanically prepared before testing and foil-strain gauges, used for a crack increment monitoring, were installed on the prepared specimens. 5 mm long, RMF A-5, foil gauges were used in testing procedure. The device for a crack increment registration, FRACTOMAT [9], was used for monitoring the crack propagation with a foil gauge. The system for a crack increment measuring, FRACTOMAT, and foil gauge register the change in electrical resistance within a foil gauge. FRACTOMAT – foil gauge operating scheme is shown in Fig. 8.

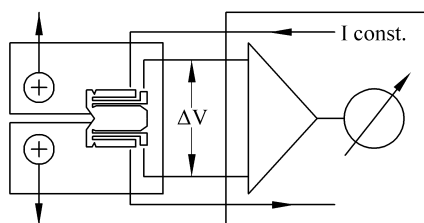


Figure 8 Foil gauge scheme and crack propagation registration method

The gauge is a thin, resistant, measuring foil installed on a specimen the same way as classic strain gauges. The appearance of the specimen prepared for the testing is shown in Fig. 9. As a fatigue crack propagates beneath the foil gauge, it reaps following the fatigue crack tip, which causes the electrical resistance of the foil to linearly alternate with the change of the crack length.

$a - N$  curves are used for the crack propagation rate determination. Calculation procedure consists of approximation in seven consecutive points with a second degree parabola, starting with the first point of  $a - N$  dependence, using the least square method [1, 10]:

$$a_I = b_0 + b_1 N + b_2 N^2, \quad (8)$$

and then the first derivative is determined in the middle point of a segment. That means that the real curve is approximated by a series of parabolas, from which the first goes through the points 1 ÷ 7, the second goes through the points 2 ÷ 8, the third goes through the points 3 ÷ 9 and further on. The crack propagation rate is determined as a derivative in the middle point (point 4 for the first parabola, 5 for the second, 6 for the third and further on) [1, 10]:

$$\frac{da}{dN} = b_1 + 2b_2 N. \quad (9)$$

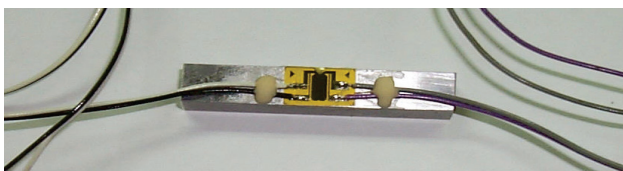


Figure 9 Appearance of the prepared specimen for testing of the fatigue crack propagation parameters

In this way the propagation rate is obtained for the first parabola [1, 10]:

$$a_I = b_{0I} + b_{1I} N_I + b_{2I} N_I^2, \quad \left. \frac{da_I}{dN_I} \right|_4 = b_{1I} + b_{2I} N_{I4}. \quad (10)$$

Propagation rates for other parabolas are determined in the same way.

Determination of the dependence of the fatigue crack propagation rate,  $da/dN$ , and the range of the stress intensity factor,  $\Delta K$ , comes down to the determination of the coefficient  $C$  and the exponent  $m$  of the Paris equation. The range of the stress intensity factor,  $\Delta K$ , which depends on the specimen geometry and crack length, and on the range of the variable force  $\Delta F = F_h -$

$F_l$ , should be ascribed to the fatigue crack propagation rate for the current crack length,  $a$ .

The following expression is used for determination of the stress intensity factor range:

$$\Delta K = \frac{\Delta F \cdot L}{B \cdot \sqrt{W^3}} \cdot f\left(\frac{a}{W}\right), \quad (11)$$

where:

$$f\left(\frac{a}{W}\right) = \frac{\sqrt[3]{\frac{a}{W}}}{2 \cdot \left(1 + 2 \cdot \frac{a}{W}\right) \cdot \left(1 - \frac{a}{W}\right)^{3/2}} \left[ 1,99 - \frac{a}{W} \cdot \left(1 - \frac{a}{W}\right) \cdot \left(2,15 - 3,93 \cdot \frac{a}{W} + 2,7 \cdot \left(\frac{a}{W}\right)^2\right) \right], \quad (12)$$

$L$  – support span,

$B$  – specimen thickness,

$W$  – specimen width (height),

$a$  – crack length.

The limit  $\Delta K_{th}$  can be determined: by gradual reduction of the load until crack propagation stops, by annealing of a notched specimen in order to eliminate residual stress around the crack tip and by gradual increment of the load until the crack propagation starts and using a specimen with the shape that is characterized by the stress intensity decrease with a crack length.

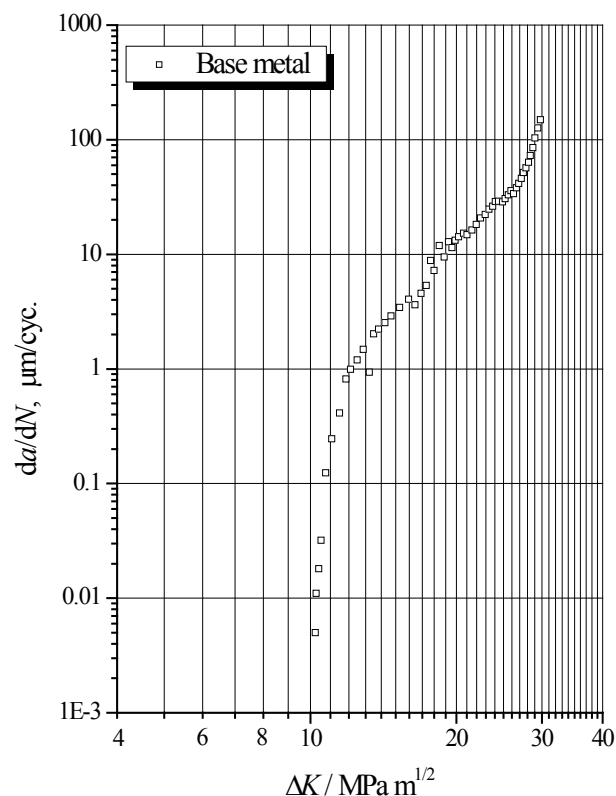


Figure 10  $da/dN - \Delta K$  dependency diagram for the BM specimen

Dependences  $\lg(da/dN) - \lg(\Delta K)$  are calculated and plotted, based on the testing progress. Diagrams of the fatigue crack propagation rate,  $da/dN$ , and the stress

intensity range alteration,  $\Delta K$ , for the tested samples are shown: in Fig. 10 for a specimen with a notch in BM, in Fig. 11 for a specimen with a notch in WM and in Fig. 12 for a specimen with a notch in HAZ [1].

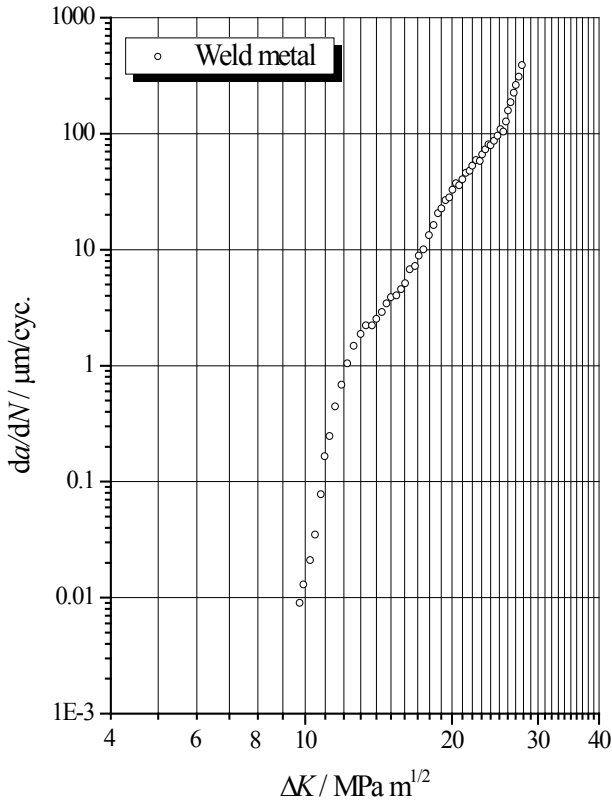


Figure 11  $da/dN - \Delta K$  dependency diagram for the WM specimen

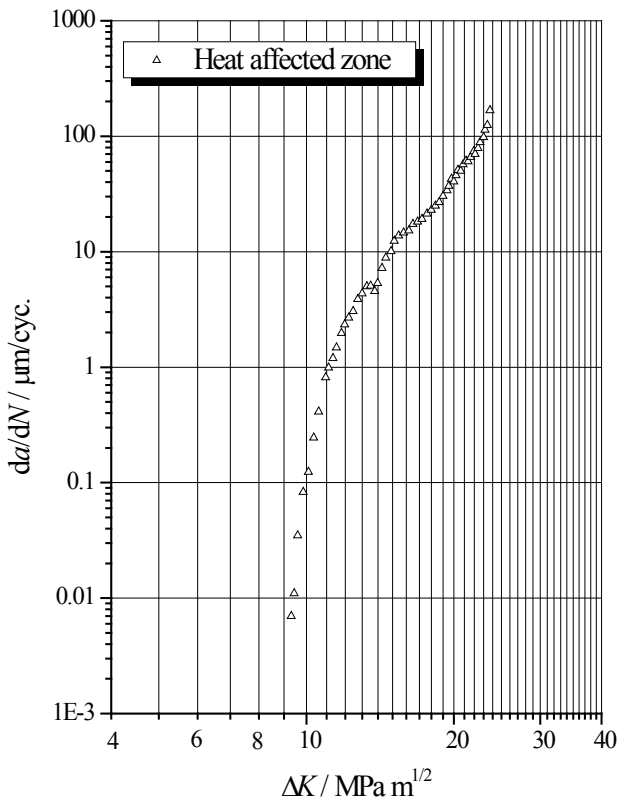


Figure 12  $da/dN - \Delta K$  dependency diagram for the HAZ specimen

Values of the coefficient  $C$  and  $m$  for the BM specimen are given in Tab. 4, for the WM specimen in Tab. 5 and for the HAZ specimen in Tab. 6 [1].

Table 4 Coefficients in Paris equation for the BM specimen

Propagation zone mark	Coefficient $C$	Coefficient $m$	$\Delta K_{th}$ / $MPa \cdot m^{1/2}$
I	$3,98 \times 10^{-14}$	4,139	10,22
III	$1,67 \times 10^{-13}$	3,765	

Table 5 Coefficients in the Paris equation for the WM specimen

Propagation zone mark	Coefficient $C$	Coefficient $m$	$\Delta K_{th}$ / $MPa \cdot m^{1/2}$
I	$8,38 \times 10^{-15}$	4,798	
II	$3,30 \times 10^{-19}$	8,462	8,45
III	$7,93 \times 10^{-15}$	5,078	

Table 6 Coefficients in the Paris equation for the HAZ specimen

Propagation zone mark	Coefficient $C$	Coefficient $m$	$\Delta K_{th}$ / $MPa \cdot m^{1/2}$
I	$1,90 \times 10^{-20}$	10,259	
II	$4,63 \times 10^{-12}$	2,667	
III	$2,90 \times 10^{-16}$	6,403	8,71
IV	$7,87 \times 10^{-13}$	3,560	
V	$1,48 \times 10^{-16}$	6,505	
VI	$1,74 \times 10^{-14}$	4,929	

### 3 Conclusion

The testing was performed on the specimens with a notch in characteristic zones of the welded joint. Heterogeneity of mechanical properties of a welded joint and its components can clearly be seen through obtained values of fracture toughness under plain strain,  $K_{Ic}$ , that is determined indirectly by  $J_{Ic}$  integral. Specimens with a notch in base metal, have the highest measured value of  $K_{Ic}$ . Specimens with a notch in HAZ have slightly lower values of  $K_{Ic}$ , however in this particular case the differences are relatively small ranging between 10 to 15  $MPa \cdot m^{1/2}$  compared to minimal and maximal value [1]. These differences do not have to have more significant influence at structures that are submitted to static load in exploitation. However, when it comes to the conditions in which structures are submitted to the constant variable load, changes of the  $K_{Ic}$  value are very significant, because critical crack length,  $a_c$ , directly depends on the value  $K_{Ic}$ . Nature of the curves only changes in dependence of a notch positioning, or a crack penetrating point. Almost identical dependence of individual curves nature in each group can be seen by analysing obtained curves. It should be noticed that the difference between specimens is only in maximal force value, which is in direct dependence on the fatigue crack length. It is noticeable that structural and mechanical heterogeneity of the welded joint has significant influence on its resistance to a crack development, both in elastic and in plastic area [1].

Welded joint toughness should be connected with the slope change of the curve part in the zone of the Paris law validity. Slower propagation is confirmed with the specimens with a crack in BM and HAZ, because for the same propagation rate it requires wider range of the stress intensity factor. Higher fatigue crack propagation rate for transition to the brittle crack area is needed for higher  $K_{Ic}$

values, which can be clearly seen in Figs. 10 to 12. By observation of the welded joint of low-alloyed steel it can be noticed that for the WM transformation rate into the brittle fracture is slightly lower compared to the BM and HAZ which is expected due to the lower value of  $K_{Ic}$  in WM [1, 11]. As it can be seen a notch positioning and crack initiation point can affect the fatigue threshold value,  $\Delta K_{th}$ , and the Paris equation parameters. It is especially pronounced in determination of the fatigue crack propagation rate in HAZ. Here we have six different changes of the fatigue crack propagation rate, which indicates the different structures a crack goes through [1, 11]. Maximal propagation rate of a fatigue crack can be expected on the level of stress intensity factor range that is forthcoming the fracture toughness under plane strain, because on that level it reaches the brittle fracture. If the value of the fracture toughness under the plane strain,  $K_{Ic}$ , is entered in Figs. 10 to 12, the propagation rate of the fatigue crack at which the fatigue process will be replaced by the development of brittle crack can be estimated, at different load levels. Worse situation will occur at higher load, because small loads cannot cause such propagation rates of a fatigue crack to approach the level of stress intensity factor that is needed for the generation of a brittle crack.

Based on the analysis of the testing results, identical behaviour of characteristic zones of the welded joint was shown in this paper, applying two different parameters.

#### 4 References

- [1] Čamagić, I. Analiza napona i deformacija zavarenih spojeva niskolegiranih čelika povišene čvrstoće u prisustvu prslina. Magistarski rad, Fakultet tehničkih nauka, Kosovska Mitrovica, 2009.
- [2] SRPS EN ISO 9692-1:2012. Welding and allied processes - Recommendations for joint preparation - Part 1: Manual metal-arc welding, gas-shielded metal-arc welding, gas welding, TIG welding and beam welding of steels (ISO 9692-1:2003).
- [3] ASTM E399-89. Standard Test Method for Plane-Strain Fracture Toughness of Metallic Materials. // Annual Book of ASTM Standards, Vol. 03.01., 1986, pp. 522.
- [4] BS 5762-DD 19. Standard Test Method for Crack Opening Displacement, London, 1976.
- [5] ASTM E813-89. Standard Test Method for  $J_{Ic}$ . A Measure of Fracture Toughness. // Annual Book of ASTM Standards, Vol. 03.01., 1993, pp. 651.
- [6] ASTM E1152-91. Standard Test Method for Determining  $J$ - $R$  Curve. // Annual Book of ASTM Standards, Vol. 03.01., 1995, pp. 724.
- [7] BS 7448-Part 1. Fracture mechanics toughness tests - Method for determination of  $K_{Ic}$  critical CTOD and critical  $J$  values of metallic materials. // BSI, 1991.
- [8] Paris, P. C.; Erdogan, F. A Critical Analysis of Crack Propagation Laws. // Journal Basic Eng. Trans. ASME. 85, 4(1963), pp. 528.
- [9] Paris, P. C.; Hayden, B. R. A New System for Fatigue Crack Growth Measurement and Control. // ASTM Symposium on Fatigue Crack Growth. Pittsburg, 1989.
- [10] Burzić, Z. Ispitivanje promenljivim opterećenjem glatkih i zarezanih epruveta. // Eksperimentalne i numeričke metode u oceni integriteta konstrukcije. 7. Tematski zbornik radova, V. Plana, 1997, pp. 75-92.
- [11] Čamagić, I.; Burzić, Z.; Cvetković, S. Primena mehanike loma u određivanju parametara rasta zamorne prslina za karakteristične oblasti zavarenog spoja. // Zavarivanje i zavarene konstrukcije. 53, 3(2008), pp. 97-103.

#### Authors' addresses

**mr Ivica Čamagić, assistant**  
Faculty of Technical Sciences  
7 Kneza Miloša Street  
Kosovska Mitrovica, Serbia  
Phone: +381 28 425 320  
Fax: +381 28 425 322  
E-mail: ivica.camagic@pr.ac.rs

**Nemanja Vasić, assistant**  
Faculty of Technical Sciences  
7 Kneza Miloša Street  
Kosovska Mitrovica, Serbia  
Phone: +381 28 425 320  
Fax: +381 28 425 322  
E-mail: nemanja.vasic@pr.ac.rs

**dr Zlatibor Vasić, professor**  
Faculty of Technical Sciences  
7 Kneza Miloša Street  
Kosovska Mitrovica, Serbia  
Phone: +381 28 425 320  
Fax: +381 28 425 322  
E-mail: zlatibor.vasic@pr.ac.rs

**dr Zijah Burzić, scientific advisor**  
Military Institute of Techniques  
1 Ratka Resanovića Street  
Belgrade, Serbia  
Phone: +381 11 250 8308  
Fax: +381 11 250 8474  
E-mail: zijah\_burzic@rvkds.net

**dr Aleksandar Sedmak, professor**  
Faculty of Mechanical Engineering  
16 Kraljice Marije Street  
Belgrade, Serbia  
Phone: +381 11 33 70 266-275  
Fax: +381 11 337 0364  
E-mail: asedmak@mas.bg.ac.rs